GEOLOGY | THE GEOLOGICAL SOCIETY OF AMERICA®

https://doi.org/10.1130/G49854.1

Manuscript received 3 March 2021
Revised manuscript received 9 November 2021
Manuscript accepted 21 January 2022

Published online 26 April 2022

Atypical landslide induces speedup, advance, and long-term slowdown of a tidewater glacier

Maximillian Van Wyk de Vries[1,2], Andrew D. Wickert[1,2], Kelly R. MacGregor[3], Camilo Rada[4] and Michael J. Willis[5]
[1]Department of Earth and Environmental Sciences, University of Minnesota, Minneapolis, Minnesota 55455, USA
[2]Saint Anthony Falls Laboratory, University of Minnesota, Minneapolis, Minnesota 55455, USA
[3]Department of Geology, Macalester College, Saint Paul, Minnesota 55105, USA
[4]Centro de Investigación GAIA Antártica, Universidad de Magallanes, 6210427 Punta Arenas, Chile
[5]Cooperative Institute for Research in Environmental Sciences (CIRES), University of Colorado, Boulder, Colorado 80309, USA

ABSTRACT

Atmospheric and oceanic warming over the past century have driven rapid glacier thinning and retreat, destabilizing hillslopes and increasing the frequency of landslides. The impact of these landslides on glacier dynamics and resultant secondary landslide hazards are not fully understood. We investigated how a 262 ± 77 × 10^6 m^3 landslide affected the flow of Amalia Glacier, Chilean Patagonia. Despite being one of the largest recorded landslides in a glaciated region, it emplaced little debris onto the glacier surface. Instead, it left a series of landslide-perpendicular ridges, landslide-parallel fractures, and an apron of ice debris—with blocks as much as 25 m across. Our observations suggest that a deep-seated failure of the mountainside impacted the glacier flank, propagating brittle deformation through the ice and emplacing the bulk of the rock mass below the glacier. The landslide triggered a brief downglacier acceleration of Amalia Glacier followed by a slowdown of as much as 60% of the pre-landslide speed and increased suspended-sediment concentrations in the fjord. These results highlight that landslides may induce widespread and long-lasting disruptions to glacier dynamics.

INTRODUCTION

Glaciers produce landslide-prone conditions (Záruba and Mencl, 1982) by eroding and oversteepening slopes, depositing unconsolidated moraines (Shulmeister et al., 2009; Shugar and Clague, 2011), and propagating bedrock fractures (Sanders et al., 2012; Grämiger et al., 2017). Ongoing global glacier retreat and thinning (Radić and Hock, 2011; Leclercq et al., 2014; Shannon et al., 2019) exposes and debuttresses these ice-marginal hillslopes (Holm et al., 2004; Fischer et al., 2006; Huggel et al., 2012; Deline et al., 2015), further increasing landslide potential.

These factors increase the likelihood of landslides onto glaciers, which may then also feed back into change in glacier dynamics and hazards. Observational (Hewitt, 1988; Gardner and Hewitt, 1990; Shugar et al., 2012; Higman et al., 2018) and geological (Santamaria Tovar et al., 2008; Vacco et al., 2010) data record or support glacier advance in response to landsliding and mine-tailings loading (Jamieson et al., 2015). A causal link between a supraglacial landslide and a glacier surge was also proposed at Bualtar Glacier, Pakistan, although it could not be confirmed through direct observations (Hewitt, 1988; Gardner and Hewitt, 1990). In an extreme case, a 2002 CE supraglacial landslide at Kolka Glacier, Russia, triggered a full glacier detachment, resulting in 125 fatalities (Haeberli et al., 2004). Landslides in supraglacial and paraglacial environments may also generate tsunamis (Blikra et al., 2006; Higman et al., 2018). We provide a new example of the effect that landslides may have on glacier dynamics through the study of a large landslide at the fast-flowing tidewater Amalia Glacier (Chilean Patagonia; 50°55′S, 73°37′W).

Amalia Glacier is a rapidly thinning, 160 km^2 tidewater glacier draining a portion of the Southern Patagonian Icefield toward the Pacific Ocean. Historical photography from 1908 CE to preset demonstrates >8 km of monotonic frontal retreat over the past century (Fig. 1). The >300 m of ice thinning associated with this retreat has exposed the unconsolidated flank of the active volcano (Harambourg, 1988) Reclus along the southern margin of Amalia Glacier, which yields a quasi-annual flux of small landslides, with larger events in 1979, in 2017, and on 26 April 2019 (Fig. 1).

We investigated the 2019 landslide, originating from the northeastern flank of Reclus volcano. We note a temporal correlation between rapid ice thinning and landslide emplacement but did not investigate causal links. We instead applied repeat satellite imagery to resolve unusual characteristics of the 2019 landslide and its impact on Amalia Glacier's dynamics.

METHODS

We use remotely sensed data to observe changes in both Amalia Glacier and the adjacent flank of Reclus volcano from 2015 to 2021. We calculated the 2019 landslide volume by subtracting a pre-event (May 2017) digital elevation model (DEM) from the earliest post-event (August 2019) DEM (see the Supplemental Material[1]). We derived a glacier-front thickness anomaly using the same DEM pair, subtracting the long-term glacier-elevation trend (calculated from the 2014 DEM to the 2017 DEM).

We used optical satellite imagery from the European Space Agency Sentinel-2 mission and the feature-tracking toolbox Glacier Image Velocimetry (GIV, https://www.maxgeohub.com/giv/; Van Wyk de Vries and Wickert, 2021) to calculate Amalia Glacier's surface velocity. Starting with 160 cloud-free Sentinel-2 images, we generated a set of all possible image pairs

[1]Supplemental Material. Additional details about Amalia Glacier's surface velocity and post-landslide evolution, rSSC and landslide volume calculations, and ISSM glacier model. Please visit https://doi.org/10.1130/GEOL.S.19424345 to access the supplemental material, and contact editing@geosociety.org with any questions.

CITATION: Van Wyk de Vries, M. et al., 2022, Atypical landslide induces speedup, advance, and long-term slowdown of a tidewater glacier: Geology, v. 50, p. 806–811, https://doi.org/10.1130/G49854.1

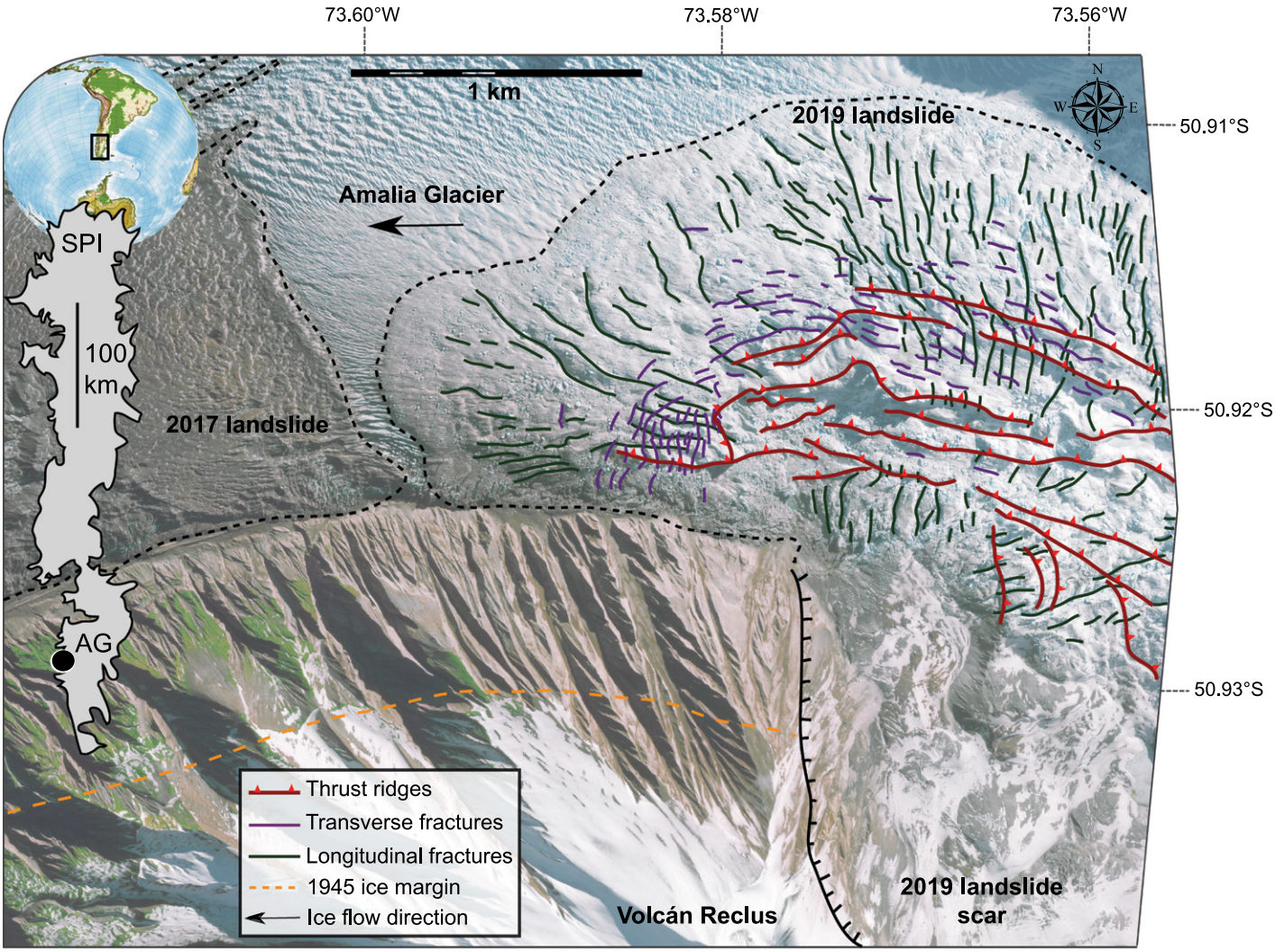

Figure 1. Location of Amalia Glacier (AG), Reclus volcano (Harambourg, 1988), and two large landslides (Southern Patagonian Icefield [SPI], southern Chile). Structural annotations are overlaid onto 23 August 2019 WorldView satellite image. Note the extensive fractures and thrust ridges in the region of the landslide emplacement. The three-dimensional model is available at https://skfb.ly/6SQwJ.

with temporal separations of between 1 week and 9 months ($n = 3459$). We then filtered and resampled the results into monthly velocity maps using a weighted averaging scheme (Van Wyk de Vries and Wickert, 2021) and difference pre- and post-landslide velocities to generate monthly speed-anomaly maps.

We calculated changes in glacier frontal position and relative suspended-sediment concentrations (rSSCs) in the fjord using all cloud-free Sentinel 2 images from October 2015 to June 2021 (71 images). We calculated maximum frontal change as the maximum change in frontal position relative to October 2015; mean frontal change by dividing the frontal area change relative to October 2015 by the fjord width; and frontal ablation rate by differencing mean frontal speed and mean frontal position change (Dryak and Enderlin., 2020). We used the radiance of Sentinel-2 band 5 (705 nm) as a proxy for rSSC through a modified version of the Ulyssys Water Quality Viewer (Zlinszky and Padányi-Gulyás, 2020).

To investigate the effect of subglacial landslide emplacement on ice velocities in a more general case, we applied the Ice-Sheet and Sea-Level System Model (ISSM, https://issm.jpl.nasa.gov/; Larour et al., 2012) to a synthetic approximation of Amalia Glacier, with a length of 10 km, width of 3 km, maximum thickness of 400 m (Carrivick et al., 2016; Millan et al., 2019), and surface slope of 3.5°. We ran a transient-stress-balance glacier model with higher-order field equations. We executed an initial 10 yr "spin up" phase (time step = 0.1 yr) to achieve steady state, followed by six scenarios (see the Supplemental Material) for another 5 yr (time step = 0.01 yr) with and without the occurrence of an $\sim 250 \times 10^6$ m^3 landslide.

RESULTS

We calculated a landslide volume of $262 \pm 77 \times 10^6$ m^3. The scar area was not glaciated at the time of collapse, so the landslide must have been predominantly composed of rock. The landslide disrupted 3.5 km^2 of Amalia Glacier's surface, although detailed inspection of high-resolution satellite imagery reveals that the ice surface is free of rock debris (see the Supplemental Material).

The landslide-disrupted region consists of a proximal zone of mixed rock and ice debris, an intermediate zone dominated by transverse ridges and radial fractures, and a distal ice-debris apron (Fig. 1). In the proximal zone, the pre-landslide glacier margin has been locally displaced >100 m, replaced by a mix of rock and ice debris. In the debris-free intermediate zone, 10–30-m-high ice ridges oriented transverse to the landslide-emplacement direction overprint the preexisting crevasse fabric (Fig. 1). Amalia Glacier's surface-fracture pattern and surface-elevation change suggest an upward and lateral displacement of the glacier ice, with the bulk of the debris emplaced at the glacier bed and margin. The distal ice-debris apron contains ice fragments as much as 25 m in size and is free

of rock debris. January 2021 Sentinel-2 imagery shows that the anomalous fracture fabric remains present 1.5 yr post-landslide, although the southern margin of Amalia Glacier has readvanced 300 m into the landslide scar.

Amalia Glacier's surface speed shows rapid changes following the landslide emplacement. Downglacier from the landslide, Amalia Glacier accelerated by as much as 400 m yr^{-1} in May 2019 (a 40% increase relative to May 2018), while the portion of Amalia Glacier upglacier of the landslide slowed by a similar magnitude (Figs. 2 and 3). In the 4 months following the landslide, the zone of increased ice-surface speed migrated downglacier and decayed. This was associated with between 15 and 90 m of ice thickening totaling 209 × 10^6 m^3—comparable to the landslide volume—and concentrated at the calving front (Fig. 3). In addition, Amalia Glacier reversed a centennial retreat trend (Fig. 1) and advanced one kilometer to its farthest extent within the past five years. Both the thickening and frontal advance continue as of June 2021, more than two years post-landslide.

For the 4 months immediately following landslide emplacement, slowdown occurred upglacier of the landslide. Between August and November 2019, the slowdown propagated through the entire glacier (Figs. 2 and 3). After November 2019, the slowdown became greatest at the glacier front, where glacier speed dropped from >1000 m yr^{-1} in June 2019 to 600–700 m yr^{-1} in November 2019 (Fig. 4). As of June 2021, ice speed in the vicinity of the landslide has recovered to within 10% of pre-collapse levels, whereas ice speed near Amalia Glacier's calving front remained slow (700 m yr^{-1} in June 2021 compared to 1175 m yr^{-1} in June 2018). Amalia Glacier's frontal ablation rate dropped by 35% in 2020 relative to pre-landslide values and remains at that level as of June 2021. The rSSC at the front of Amalia Glacier peaked at more than five times the pre-landslide maximum in austral summer 2020 and 2021 (Fig. 2C).

In the simulated glacier model, landslide emplacement increases ice-surface speed downglacier of the landslide center by ~600 m yr^{-1} and reduces it by ~250 m yr^{-1} upglacier (Fig. 4). Two years after the landslide, the modeled glacier remains ~100 m yr^{-1} slower near the zone of landslide emplacement. A model run with a 20% increase in basal friction shows a similar overall trend, with a further ~200 m yr^{-1} glacier-wide slowdown.

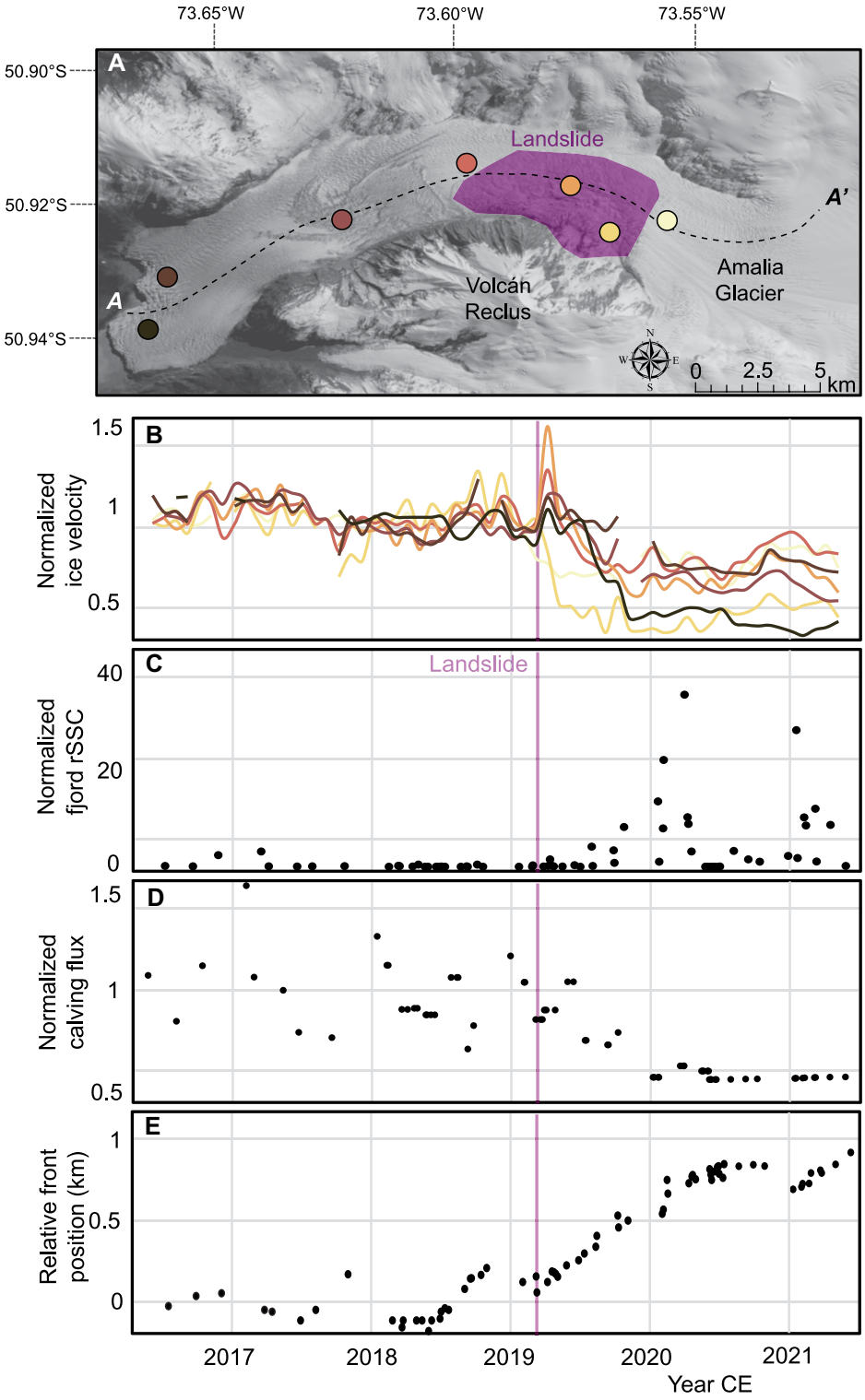

Figure 2. Changes induced by the April 2019 landslide on Amalia Glacier, Chilean Patagonia. (A) Map of Amalia Glacier, showing points where we extracted velocity time series (B) and centerline used in Figure 3. (B–D) Changes in glacier surface velocity, rSSC, and calving flux normalized to the pre-landslide mean. (E) Maximum frontal position relative to October 2015 (see the Supplemental Material [see footnote 1]).

DISCUSSION

The landslide-induced dynamic glacier changes may relate to changes in the stress field, frontal conditions, or basal hydrology, or some combination of these factors. Immediately following the landslide event, the glacier decelerated upglacier and accelerated downglacier of the landslide center. The synthetic glacier model, which does not account for any change in basal friction, basal hydrology, or calving-front conditions (Figs. 4E–4H), exhibits a similar speed-anomaly pattern for the first 3 months following landslide emplacement. Disruptions to the ice-surface and basal topography alone provide a viable mechanism for the short-term post-landslide downglacier acceleration at Amalia Glacier.

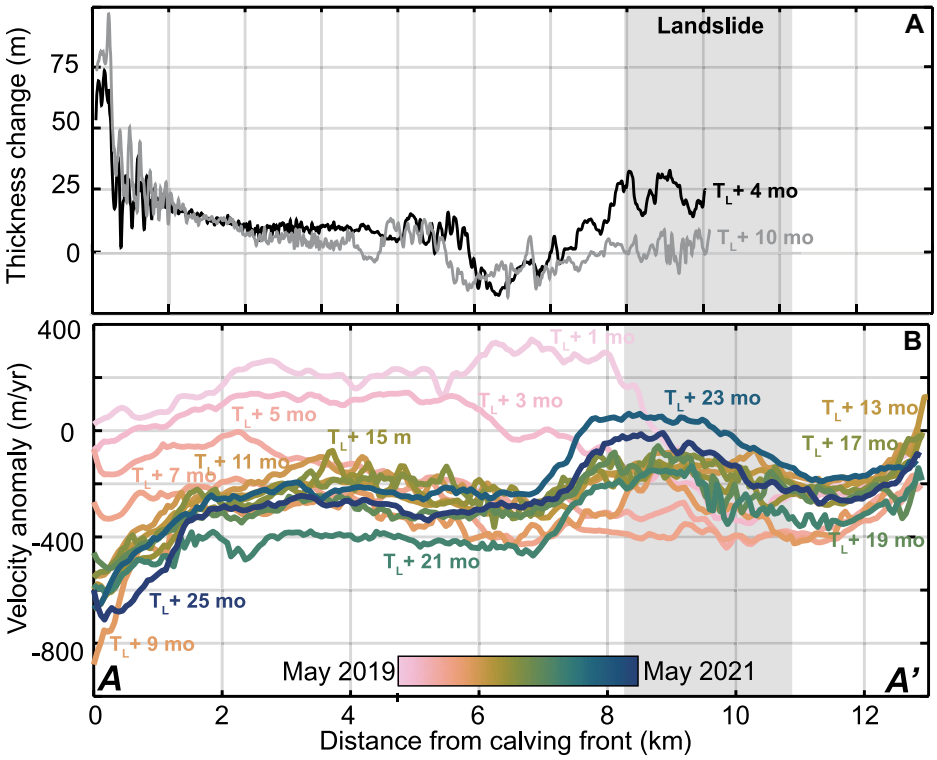

Figure 3. Detrended May 2017–August 2019 (4 months post-landslide) and May 2017–February 2020 (10 months post-landslide) changes in Amalia Glacier (Chilean Patagonia) ice thickness (A) and ice-surface velocity anomaly (B) along the glacier centerline (shown in Fig. 2A). Velocities are shown every 2 months. T_L is time of landslide emplacement.

Starting at ~3 months following the landslide, slowdown of ice surface speed increased in magnitude and propagated downglacier. The focus of the slowdown was first located at the zone of landslide emplacement, followed by a switch to the glacier calving front after 9 months. Changes in driving stresses alone, as represented by our model outputs, cannot explain this longer-term slowdown and its pattern.

One explanation for the slowdown could be a change in basal hydrology. An increase in the efficiency of subglacial drainage reduces subglacial water pressure, increases basal friction, and lowers ice speed (Iken and Truffer, 1997; Cuffey and Paterson, 2010). Without direct measurements of Amalia Glacier's subglacial conditions, we examine fjord rSSC as a proxy. Glacier sediment export is controlled by the availability of subglacial sediment and the subglacial drainage system's sediment-transport capacity, with the latter being higher in efficient (i.e., internally connected) drainage systems.

We observed high rSSC in the Amalia Fjord during austral summer 2020 and summer 2021 (Fig. 2) when compared to prior summers, including the period following the 2017 supraglacial landslide. Times of highest rSSC coincide with the melt season. The 2019 landslide injected large quantities of loose sediment at the base of Amalia Glacier while also locally disrupting englacial and supraglacial fracture networks. This latter effect may have changed subglacial flow paths, allowing sediment to be sourced from new areas of the glacier bed (e.g., Anderson et al., 1999). In addition, any increase in the efficiency of Amalia Glacier's subglacial drainage system could explain the initial 9 month slowdown centered on the zone of landslide emplacement. We cannot, however, distinguish the relative contributions of increased drainage efficiency and greater sediment availability to the observed increase in rSSC.

Conversion of a formerly marine-terminating glacier to a land-terminating glacier increases its basal friction, thereby reducing its speed at the ice front. This buttressing at the terminus may consequently reduce ice speeds upglacier. Amalia Glacier's southern ice front slowed 40% when a delta formed ~9 months post-landslide, and portions of its terminus became land-terminating. Amalia Glacier continues to advance as of November 2021, and its calving flux has remained at approximately two-thirds of its pre-landslide value since early 2020.

In summary, we ascribe Amalia Glacier's speed changes to three sources: (1) topographically induced changes in the glacier's stress field, related to subglacial landslide emplacement and uplift of the ice surface; (2) a reduction in basal slip related to more efficient meltwater evacuation and consequent depressurization of the subglacial hydrological system; and (3) proglacial delta formation and partial grounding of Amalia Glacier's ice front. Our results highlight the potential of remote sensing for understanding glacier dynamic changes in remote areas, although field data would be valuable for better assessing glacier basal processes and stress changes.

Certain characteristics of Amalia Glacier's response to the emplacement of a large landslide are reminiscent of glacier surges. In a typical surge-type glacier, ice gradually accumulates in a reservoir zone until it reaches a critical level, before destabilizing and rapidly draining downglacier during the surge (Eisen et al., 2001, 2005). At Amalia Glacier, landslide emplacement instantaneously formed a "reservoir zone" by uplifting the ice surface and drove rapid downglacier thickening and acceleration (Figs. 2 and 3). The long-term (2 + yr) frontal slowdown and proglacial delta formation are more reminiscent of the advance phase of a tidewater glacier, where a shallow proglacial shoal reduces frontal ablation and enables glacier advance (Post et al., 2011). Future studies of Amalia Glacier are needed to evaluate whether the disruption is temporary or the glacier has shifted into a new steady state.

The hazard related to this glacier response at Amalia Glacier is minor due to its remoteness. However, large-magnitude, rapid, and long-term changes in glacier dynamics may be of concern in more populated regions (e.g., Gardner and Hewitt, 1990; Deline et al., 2015). Our results underscore the importance of glacier-related landslide monitoring, including how interactions between landslides and glacier dynamics may extend the effects of a landslide many kilometers beyond its runout zone.

CONCLUSIONS

A $262 \pm 77 \times 10^6$ m^3 landslide impacted Amalia Glacier on 26 April 2019. Unusually, this landslide deposited little to no debris on the glacier surface but instead displaced the glacier margin, thickened the glacier through brittle faulting and accretion of eroded ice debris, and imprinted a strong brittle-contractional fracture pattern. Remotely sensed glacier-surface speed and DEMs show that Amalia Glacier accelerated by 100–400 m yr^{-1}, thickened by 10–50 m, and advanced more than 1 km following the landslide. This acceleration was succeeded by glacier-wide slowdown, centered first on the landslide runout zone and then on Amalia Glacier's calving front. We ascribe this complex spatiotemporal change in glacier speed to three factors: (1) a change in driving stresses, related to the altered ice-surface and basal topography; (2) a shift in glacier basal hydrology, with the landslide increasing basal drainage-network efficiency; and (3) increased glacier-front stability due to proglacial delta formation and grounding of the ice front. Two years after the landslide,

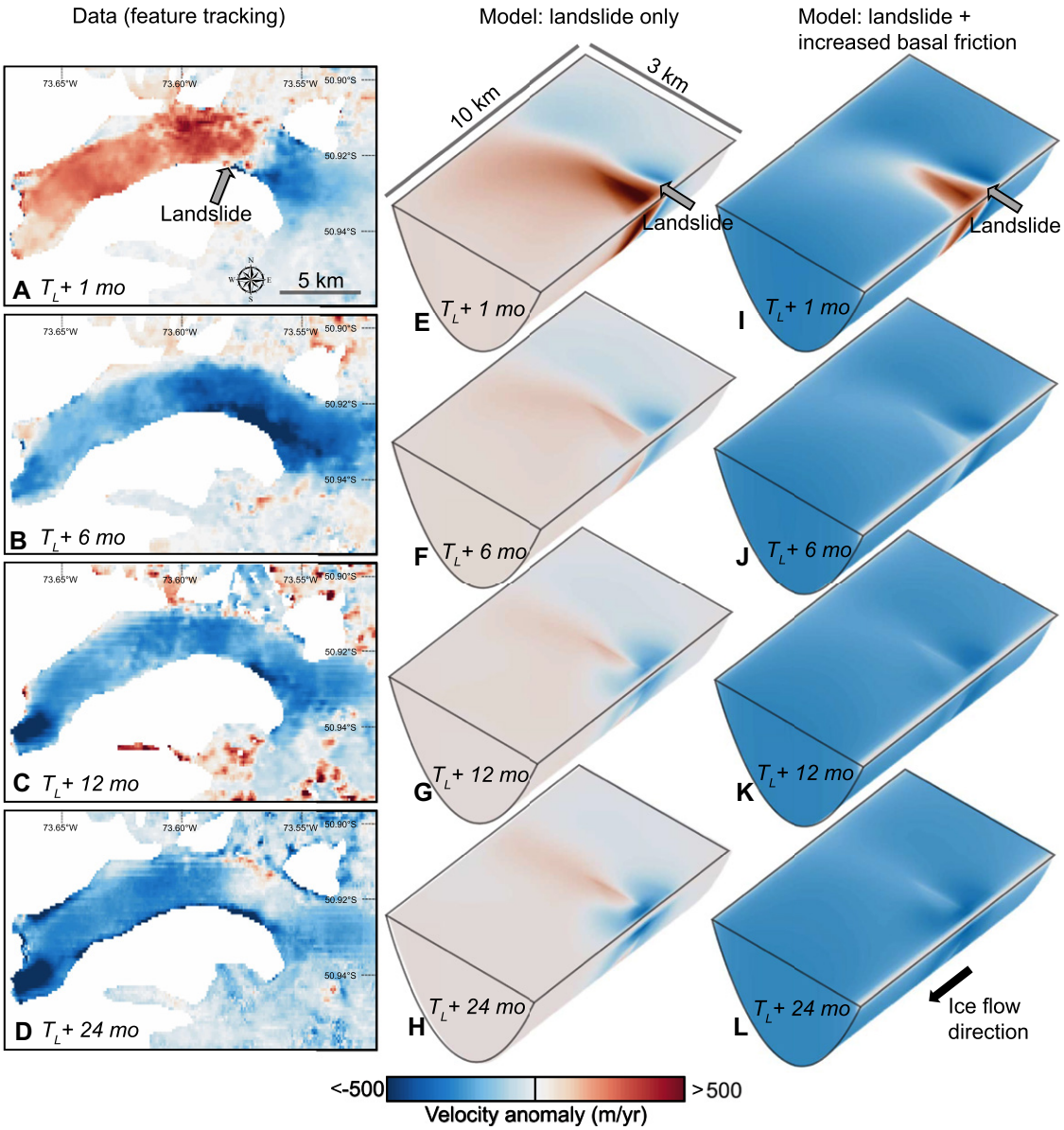

Figure 4. Post-landslide ice-surface velocity anomaly. Panels A–D show real data; E–H show Ice-Sheet and Sea-Level System Model (ISSM, https://issm.jpl.nasa.gov/; Larour et al., 2012) outputs with only landslide emplacement; and I–L show model outputs with both landslide emplacement and increase in basal friction. T_L is time of landslide emplacement.

frontal speed and calving flux remain suppressed. These results highlight that landslides, forecast to increase in frequency with climatic warming, can alter the dynamics of even very large glaciers.

ACKNOWLEDGMENTS

Van Wyk de Vries has been supported by the University of Minnesota College of Science and Engineering and a Doctoral Dissertation Fellowship. This work is supported by U.S. National Science Foundation grant EAR-1714614 to Wickert, E. Ito, and A. Noren, and lead Principal Investigator M.B. Magnani. Imagery was provided by the European Space Agency (proposal N57129). Reviews by K. Cuffey, F. Beaud, and M. Truffer guided revisions that improved the quality of the manuscript, the focus of our modeling, and our placement of this event in its scientific context.

REFERENCES CITED

Anderson, S.P., Fernald, K.M.H., Anderson, R.S., and Humphrey, N.F., 1999, Physical and chemical characterization of a spring flood event, Bench Glacier, Alaska, U.S.A.: Evidence for water storage: Journal of Glaciology, v. 45, p. 177–189, https://doi.org/10.1017/S0022143000001684.

Blikra, L.H., Longva, O., Braathen, A., Anda, E., Dehls, J.F., and Stalsberg, K., 2006, Rock slope failures in Norwegian fjord areas: Examples, spatial distribution and temporal pattern, *in* Evans, S.G., et al., eds., Landslides from Massive Rock Slope Failure: Dordrecht, Springer, p. 475–496, https://doi.org/10.1007/978-1-4020-4037-5_26.

Carrivick, J.L., Davies, B.J., James, W.H.M., Quincey, D.J., and Glasser, N.F., 2016, Distributed ice thickness and glacier volume in southern South America: Global and Planetary Change, v. 146, p. 122–132, https://doi.org/10.1016/j.gloplacha.2016.09.010.

Cuffey, K.M., and Paterson, W.S.B., 2010, The Physics of Glaciers (fourth edition): Amsterdam, Academic Press, 721 p.

Deline, P., Hewitt, K., Reznichenko, N., and Shugar, D., 2015, Rock avalanches onto glaciers, *in* Shroder, J.F., and Davies, T., eds., Landslide Hazards, Risks, and Disasters: Boston, Academic Press, p. 263–319, https://doi.org/10.1016/B978-0-12-396452-6.00009-4.

Dryak, M.C., and Enderlin, E.M., 2020, Analysis of Antarctic Peninsula glacier frontal ablation rates with respect to iceberg melt-inferred variability in ocean conditions: Journal of Glaciology, v. 66, p. 457–470, https://doi.org/10.1017/jog.2020.21.

Eisen, O., Harrison, W.D., and Raymond, C.F., 2001, The surges of Variegated Glacier, Alaska, U.S.A., and their connection to climate and mass balance: Journal of Glaciology, v. 47, p. 351–358, https://doi.org/10.3189/172756501781832179.

Eisen, O., Harrison, W.D., Raymond, C.F., Echelmeyer, K.A., Bender, G.A., and Gorda, J.L.D., 2005, Variegated Glacier, Alaska, USA: A century of surges: Journal of Glaciology, v. 51, p. 399–406, https://doi.org/10.3189/172756505781829250.

Fischer, L., Kääb, A., Huggel, C., and Noetzli, J., 2006, Geology, glacier retreat and permafrost degradation as controlling factors of slope instabilities in a high-mountain rock wall: The Monte Rosa east face: Natural Hazards and Earth System Sciences, v. 6, p. 761–772, https://doi.org/10.5194/nhess-6-761-2006.

Gardner, J.S., and Hewitt, K., 1990, A surge of Bualtar Glacier, Karakoram Range, Pakistan: A possible landslide trigger: Journal of Glaciology,

v. 36, p. 159–162, https://doi.org/10.1017/S0022143000009394.
Grämiger, L.M., Moore, J.R., Gischig, V.S., Ivy-Ochs, S., and Loew, S., 2017, Beyond debuttressing: Mechanics of paraglacial rock slope damage during repeat glacial cycles: Journal of Geophysical Research: Earth Surface, v. 122, p. 1004–1036, https://doi.org/10.1002/2016JF003967.
Haeberli, W., Huggel, C., Kääb, A., Zgraggen-Oswald, S., Polkvoj, A., Galushkin, I., Zotikov, I., and Osokin, N., 2004, The Kolka-Karmadon rock/ice slide of 20 September 2002: An extraordinary event of historical dimensions in North Ossetia, Russian Caucasus: Journal of Glaciology, v. 50, p. 533–546, https://doi.org/10.3189/172756504781829710.
Harambour, S.M., 1988, Sobre el hallazgo del mitico volcan Reclus, ex Mano del Diablo, Hielo Patagonico Sur, Magallanes, Chile: Andean Geology, v. 15, p. 173–179.
Hewitt, K., 1988, Catastrophic landslide deposits in the Karakoram Himalaya: Science, v. 242, p. 64–67, https://doi.org/10.1126/science.242.4875.64.
Higman, B., et al., 2018, The 2015 landslide and tsunami in Taan Fiord, Alaska: Scientific Reports, v. 8, 12993, https://doi.org/10.1038/s41598-018-30475-w.
Holm, K., Bovis, M., and Jakob, M., 2004, The landslide response of alpine basins to post–Little Ice Age glacial thinning and retreat in southwestern British Columbia: Geomorphology, v. 57, p. 201–216, https://doi.org/10.1016/S0169-555X(03)00103-X.
Huggel, C., Clague, J.J., and Korup, O., 2012, Is climate change responsible for changing landslide activity in high mountains?: Earth Surface Processes and Landforms, v. 37, p. 77–91, https://doi.org/10.1002/esp.2223.
Iken, A., and Truffer, M., 1997, The relationship between subglacial water pressure and velocity of Findelengletscher, Switzerland, during its advance and retreat: Journal of Glaciology, v. 43, p. 328–338, https://doi.org/10.1017/S0022143000003282.
Jamieson, S.S.R., Ewertowski, M.W., and Evans, D.J.A., 2015, Rapid advance of two mountain glaciers in response to mine-related debris loading: Journal of Geophysical Research: Earth Surface, v. 120, p. 1418–1435, https://doi.org/10.1002/2015JF003504.
Larour, E., Seroussi, H., Morlighem, M., and Rignot, E., 2012, Continental scale, high order, high spatial resolution, ice sheet modeling using the Ice Sheet System Model (ISSM): Journal of Geophysical Research: Earth Surface, v. 117, F1, https://doi.org/10.1029/2011JF002140.
Leclercq, P.W., Oerlemans, J., Basagic, H.J., Bushueva, I., Cook, A.J., and Le Bris, R., 2014, A data set of worldwide glacier length fluctuations: The Cryosphere, v. 8, p. 659–672, https://doi.org/10.5194/tc-8-659-2014.
Millan, R. et al., 2019, Ice thickness and bed elevation of the Northern and Southern Patagonian Icefields: Geophysical Research Letters, v. 46, p. 6626–6635, https://doi.org/10.1029/2019GL082485.
Post, A., O'Neel, S., Motyka, R.J., and Streveler, G., 2011, A complex relationship between calving glaciers and climate: Eos (Transactions, American Geophysical Union), v. 92, p. 305–306, https://doi.org/10.1029/2011EO370001.
Radić, V., and Hock, R., 2011, Regionally differentiated contribution of mountain glaciers and ice caps to future sea-level rise: Nature Geoscience, v. 4, p. 91–94, https://doi.org/10.1038/ngeo1052.
Sanders, J.W., Cuffey, K.M., Moore, J.R., MacGregor, K.R., and Kavanaugh, J.L., 2012, Periglacial weathering and headwall erosion in cirque glacier bergschrunds: Geology, v. 40, p. 779–782, https://doi.org/10.1130/G33330.1.
Santamaria Tovar, D., Shulmeister, J., and Davies, T.R., 2008, Evidence for a landslide origin of New Zealand's Waiho Loop moraine: Nature Geoscience, v. 1, p. 524–526, https://doi.org/10.1038/ngeo249.
Shannon, S., Smith, R., Wiltshire, A., Payne, T., Huss, M., Betts, R., Caesar, J., Koutroulis, A., Jones, D., and Harrison, S., 2019, Global glacier volume projections under high-end climate change scenarios: The Cryosphere, v. 13, p. 325–350, https://doi.org/10.5194/tc-13-325-2019.
Shugar, D.H., and Clague, J.J., 2011, The sedimentology and geomorphology of rock avalanche deposits on glaciers: Sedimentology, v. 58, p. 1762–1783, https://doi.org/10.1111/j.1365-3091.2011.01238.x.
Shugar, D.H., Rabus, B.T., Clague, J.J., and Capps, D.M., 2012, The response of Black Rapids Glacier, Alaska, to the Denali earthquake rock avalanches: Journal of Geophysical Research, v. 117, F01006, https://doi.org/10.1029/2011JF002011.
Shulmeister, J., Davies, T.R., Evans, D.J.A., Hyatt, O.M., and Tovar, D.S., 2009, Catastrophic landslides, glacier behaviour and moraine formation—A view from an active plate margin: Quaternary Science Reviews, v. 28, p. 1085–1096, https://doi.org/10.1016/j.quascirev.2008.11.015.
Vacco, D.A., Alley, R.B., and Pollard, D., 2010, Glacial advance and stagnation caused by rock avalanches: Earth and Planetary Science Letters, v. 294, p. 123–130, https://doi.org/10.1016/j.epsl.2010.03.019.
Van Wyk de Vries, M., and Wickert, A.D., 2021, Glacier Image Velocimetry: An open-source toolbox for easy and rapid calculation of high-resolution glacier-velocity fields: The Cryosphere, v. 15, p. 2115–2132, https://doi.org/10.5194/tc-15-2115-2021.
Záruba, Q., and Mencl, V., 1982, Landslides and Their Control: Amsterdam, Elsevier, 325 p.
Zlinszky, A., and Padányi-Gulyás, G., 2020, Ulyssys Water Quality Viewer: https://github.com/sentinel-hub/custom-scripts/tree/master/sentinel-2/ulyssys_water_quality_viewer.

Printed in USA